International Journal of Mass Spectrometry 285 (2009) 131–136

Contents lists available at ScienceDirect

International Journal of Mass Spectrometry

journal homepage: www.elsevier.com/locate/ijms

Unusual features in electron attachment to chlorodifluoroacetic acid ($CClF_2COOH$): Strong dissociative electron attachment near 0 eV and associative attachment at 0.75 eV

Janina Kopyra [a,b,*], Constanze König-Lehmann [b], Iwona Szamrej [a], Eugen Illenberger [b]

[a] Department of Chemistry, University of Podlasie, 3 Maja 54, 08-110 Siedlce, Poland
[b] Institut für Chemie und Biochemie, Physikalische und Theoretische Chemie, Freie Universität Berlin, Takustrasse 3, D-14195 Berlin, Germany

ARTICLE INFO

Article history:
Received 20 April 2009
Received in revised form 18 May 2009
Accepted 20 May 2009
Available online 27 May 2009

Keywords:
Dissociative electron attachment
Chlorodifluoroacetic acid
Thermal electron attachment rate constant
Mass spectrometry

ABSTRACT

Electron attachment to gas phase $CClF_2COOH$ (M) under collision free conditions exhibits very unusual features as the non-decomposed parent anion M^- (associative attachment) is observed on the mass spectrometric time scale at a resonance located at 0.75 eV while strong dissociative electron attachment (DEA) reactions already occur within a resonant feature close to 0 eV. Long lived parent anions M^- are usually only formed (if at all) at energies close to 0 eV and when no DEA channels are energetically accessible. The two by far dominant DEA reactions are due to the cleavage of the C–Cl bond with the excess charge localised on either of the fragments to form the closed shell anions CF_2COOH^- or Cl^-. Electron attachment near 0 eV also leads to more complex DEA reactions like the loss of HF or CF_2, etc., which are associated with substantial geometrical and electronic rearrangement. The thermal attachment rate constant is derived by means of an electron swarm experiment as $k = 1.5 \times 10^{-10}$ cm^3 molec.$^{-1}$ s^{-1}.

1. Introduction

Electron attachment to organic acids like formic acid (HCOOH) [1], acetic acid (CH_3COOH) [2] or the amino acid glycine (CH_2NH_2COOH) [3] is characterised by a pronounced resonance at low energy peaking between 1.2 and 1.5 eV as observed in dissociative electron attachment (DEA). This low energy transient negative ion (TNI) decomposes by the loss of a neutral hydrogen atom thereby forming the complementary closed shell anion $RCOO^-$, also assigned as $(M–H)^-$. Isotope labelling in formic acid demonstrated that H loss exclusively originates from the OH site [4]. For gas phase dissociation such selectivity cannot *a prori* be expected, as the O–H bond dissociation energy approximately equals that of C–H [5]. On the other hand, an exploration of the $(HCO_2)^-$ potential energy surface revealed that the structure $HCOO^-$ is appreciably more stable than $COOH^-$ [6,7]. Loss of neutral hydrogen via dissociative electron attachment (DEA) is hence energetically more favourable at the O–H site. Calculations assigned the low energy feature as a shape resonance of π^* COOH character [8,9]. From a detailed study of the dissociation dynamics [9] it was predicted that H loss is an intrinsically polyatomic reaction. Symmetry constraints dictate a deformation of the TNI to a non-planar geometry thereby providing the π^*/σ^* coupling in order to decompose. More specifically, initial stretching of the C=O and the C–O bond followed by a rotation of the C–H bond finally results in breaking of the O–H bond.

On the other hand, a study on vibrational excitation of the OH stretching mode in HCOOH [10] provides compelling arguments that the low energy resonance is of σ^*(OH) character. In fact, a very recent application of the resonant R-matrix theory on formic acid and glycine [11] could consistently describe all experimental observations by attributing low energy DEA via a σ^*(OH) resonance, however, at extreme conditions with respect to the energy and width (autodetachment lifetime) of the resonance. The important point is, that not the region near the equilibrium geometry of the neutral system is essential for the DEA signal, but the area near the crossing point between the neutral and anionic potential energy surface with strong contributions of non-local effects.

In trifluoroacetic acid (CF_3COOH) the situation changes appreciably [12] as now the position of the shape resonance is lowered to about 0.5 eV and in addition to the loss of H the loss of HF (generating CF_2COO^-) is observed as the second prominent decomposition channel. At ambient pressure and under the condition of supersonic beam expansions, organic acids tend to form the cyclic hydrogen bridged dimers. Electron attachment to these dimers in the gas phase show very interesting properties like an increase in the electron capture cross-section [12,13], surprisingly complex reactions triggered by slow electrons like the loss of neutral water molecules from the dimer of trifluoroacetic acid [14] or the extraordinary

* Corresponding author at: Department of Chemistry, University of Podlasie, 3 Maja 54, 08-110 Siedlce, Poland. Tel.: +48 025 6431136.
E-mail address: kopyra@ap.siedlce.pl (J. Kopyra).

1387-3806/$ – see front matter © 2009 Elsevier B.V. All rights reserved.
doi:10.1016/j.ijms.2009.05.006

ability of formic acid dimers to thermalise electrons with initial energies in the range 1–2 eV via inelastic scattering [15].

In this contribution we present a cooperative study between two laboratories (Siedlce and Berlin) to study electron attachment to chlorodifluoroacetic acid ($CClF_2COOH$). In the Siedlce laboratory the attachment rate constant for thermal electrons is derived using a newly established swarm experiment. In the Berlin laboratory, the decomposition channels of the transient negative anion (TNI) are explored using a crossed electron-molecular beams set-up. The compound shows interesting and unexpected features as now hydrogen loss is strongly suppressed and most of the ion intensity is channelled in two complementary fragment ions $(CF_2COOH)^-$ and Cl^- arising from the cleavage of the C–Cl bond with the excess charge localised on either of the two fragment. While these DEA reactions occur at electron energies close to 0 eV, the non-decomposed parent anion M^- is observed at a second resonance located at 0.75 eV. On a lower intensity scale, negative ions arising from remarkably complex reactions are observed already near 0 eV, like the loss of neutral HF or CF_2 which requires substantial electronic and geometrical rearrangement in the TNI.

2. Experimental

2.1. Electron swarm experiment

A pulsed Townsend (PT) technique for studying electron attachment processes has been applied at the Siedlce laboratory that was described in detail previously [16]. The main part of the experimental set-up consists of a cylindrical chamber with two parallel electrodes, which are stainless-steel disks of 6 cm in diameter and separated by a distance of 1.5 cm. In this technique the electron swarm is photoelectrically produced using a 5 ns Nd:YAG laser operating on fourth harmonic (266 nm) at a frequency of 10 Hz. In the presence of the buffer gas CO_2 the generated photoelectrons very quickly reach a steady-state equilibrium energy distribution.

The PT method is based on the observation of the displacement current due to electrons drifting across a parallel plate discharge gap under a homogeneous electric field E. Traversing electrons induce a change of the anode potential which increases linearly as electrons move to the collecting electrode in the pure buffer gas. In the mixture of electron acceptor and buffer gas the electrons are captured and the increase of the potential is no longer linear. The thermal electron attachment rate constant is then determined from the shape of the pulse of the temporal variation of the anode potential.

The $CClF_2COOH$–CO_2 gas mixtures were prepared inside the chamber by first injecting the minority gas and then introducing the buffer gas to obtain the highest, total pressures of the gas mixtures of 2×10^{19} molec. cm^{-3}. A number of 100 pulses were registered for a given density reduced electric field value (E/N) and then averaged and analyzed. The procedure was repeated for several E/N values in the range of $(1–4) \times 10^{-17}$ V cm^2 molec.$^{-1}$ (where electrons in carbon dioxide are in thermal equilibrium with gas molecules). Subsequently, the mixture was pumped-out to a lower pressure and the procedure was repeated for a few consecutive densities in the range of around 2×10^{19} to 8.3×10^{18} molec. cm^{-3} corresponding to pressures in the range between about 820–340 mbar.

CO_2 with a quoted purity of 99.998% was provided by Fluka Co. and was used as delivered. $CClF_2COOH$ (Sigma–Aldrich, 98%) was used after degassing by vacuum freeze-pump-thaw technique with liquid nitrogen.

2.2. Electron beam experiment

The DEA experiments were carried out at the Berlin laboratory by means of a crossed electron-molecular beams apparatus that has already been described in detail elsewhere [17]. In brief an incident electron beam of well-defined energy (FWHM ≈ 0.2 eV, electron current ≈ 10 nA) generated from a trochoidal electron monochromator [18] orthogonally intersects with an effusive molecular beam of $CClF_2COOH$. The sample is solid/liquid under ambient conditions (melting temperature 20–23 °C) and was directly deposited into a small vessel inside the vacuum system. The vessel itself is directly connected with the reaction zone by a capillary. The overall system can be heated by two *in vacuo* halogen bulbs. For the present experiments, extra heating was not necessary, as the temperature of the vessel under the operating conditions (35 °C) was sufficient to generate an effusive molecular beam of $CClF_2COOH$ emanating from the capillary. The pressure reading at one of the flanges was in the range 4×10^{-6} mbar, the background pressure in the UHV system (no sample) is in the 10^{-8} mbar range.

Negative ions formed via electron–molecule collisions are extracted from the reaction volume towards a quadrupole mass analyzer, and are detected by a single pulse counting technique. The yield of a particular anion is then recorded as a function of the incident electron energy and assigned as the ion yield function. The electron energy scale is calibrated by measuring the formation of SF_6^- ions, which exhibits a sharp peak located near 0 eV.

$CClF_2COOH$ was obtained from Sigma–Aldrich at a stated purity of 98% and used as delivered.

Under ambient pressure and temperature organic acids have a tendency to form the cyclic hydrogen bridged dimers. Under both experimental conditions, however, the presence of dimers is expected to be low or negligible due to the correspondingly low pressures. In the case of formic acid, the molar fraction of dimers at 1 mbar was calculated from the equilibrium constant [19] as 11% [15]. In the swarm experiment the partial pressure is at least one order of magnitude lower (see below).

In the beam experiment the monomers are evaporated directly into a single collision environment and dimer formation can be excluded which is consistent with the observation of M^- as the ion of highest mass.

3. Results and discussion

3.1. Electron attachment rate constant

In the swarm experiments performed at the Siedlce laboratory, the thermal rate constant for electron attachment to $CClF_2COOH$ molecules has been measured at $T = 298 \pm 0.5$ K in a sequence of experiments with constant electron acceptor-to-buffer gas concentration ratio but at different absolute pressures. T refers to both the gas temperature and the electron temperature. The concentration of the electron acceptor gas used in the experiments depends on the ability of the molecule to capture thermal electrons. In our version of the PT technique we chose conditions to get a rate of the electron disappearance from the swarm of around 10^5 s^{-1}. Therefore the applied initial concentrations of $CClF_2COOH$ were chosen to be in the range of 10^{15} molec. cm^{-3}. In the experimental procedure the saturated vapour pressure of $CClF_2COOH$ (several mbar) was reduced to around 0.5 mbar and then injected into the static chamber until concentrations in the range 10^{15} molec. cm^{-3} was established. We performed two series of measurements, one at an initial concentration of 2.9×10^{15} molec. cm^{-3} and a second at 3.3×10^{15} molec. cm^{-3}, corresponding to pressures in the range 10^{-1} mbar. Then the buffer gas CO_2 at a concentration of 2×10^{19} molec. cm^{-3} was added and the series of measurement at different absolute pressures but constant ratio between buffer and scavenging gas was performed.

Fig. 1 shows the results obtained from the two different initial concentrations of the attaching gas after averaging yielding

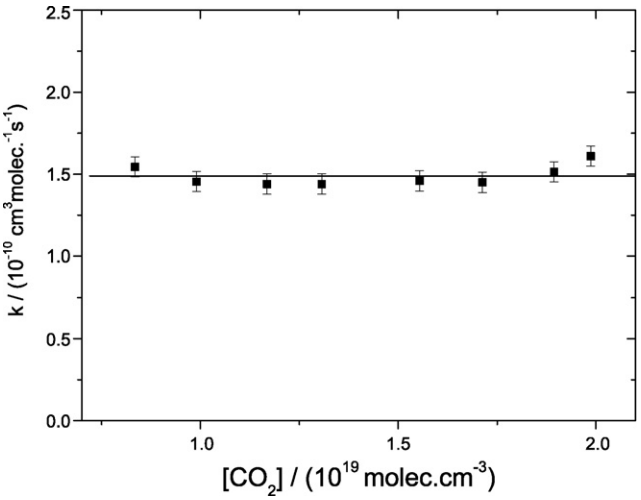

Fig. 1. Dependence of the rate constant k for the attachment of thermal electrons to $CClF_2COOH$ at different gas concentrations.

a rate constant of $k = (1.5 \pm 0.1) \times 10^{-10}$ cm^3 molec.$^{-1}$ s^{-1} for electron attachment to $CClF_2COOH$ at 298 K. The fact that the rate constant is independent of the pressure indicates, that only two body processes take place, i.e., the electrons interact with single $CClF_2COOH$ molecules. To our knowledge, for the organic acids or their halo-derivatives there are so far no literature data available for the electron attachment rate constant. The k values for halogenated hydrocarbons, *e.g.*, strongly increase with the number of chlorine atoms. In that respect, the presently derived k value, is about three orders of magnitude above those in the chlorofluorocarbons which contain one Cl atom such as CHF_2Cl or CH_3CF_2Cl [20,21] but still about three orders of magnitude below that of SF_6 which possesses one of the largest attachment rates (s-wave attachment) for thermal electrons, namely $k = 2.25 \times 10^{-7}$ cm^3 molec.$^{-1}$ s^{-1} [22].

3.2. Decomposition pathways

Figs. 2–5 show ion yields obtained from electron attachment to the target compound in the energy range 0–12 eV in absolute count rates. In Fig. 2 the two (by far) dominant products CF_2COOH^- and Cl^- arising from the cleavage of the C–Cl bond are plotted.

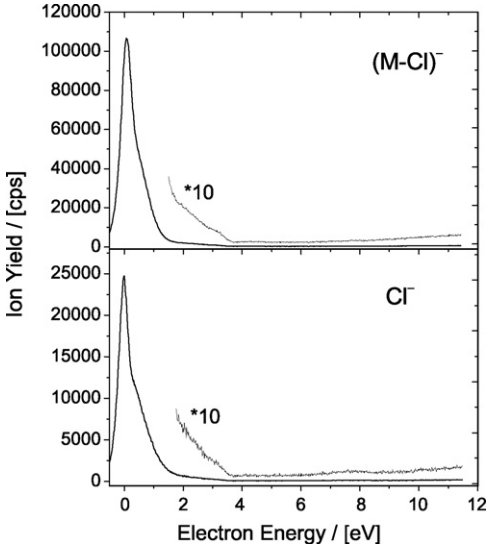

Fig. 2. Yields for the complementary ions $(M–Cl)^-$ and Cl^- from chlorodifluoroacetic acid.

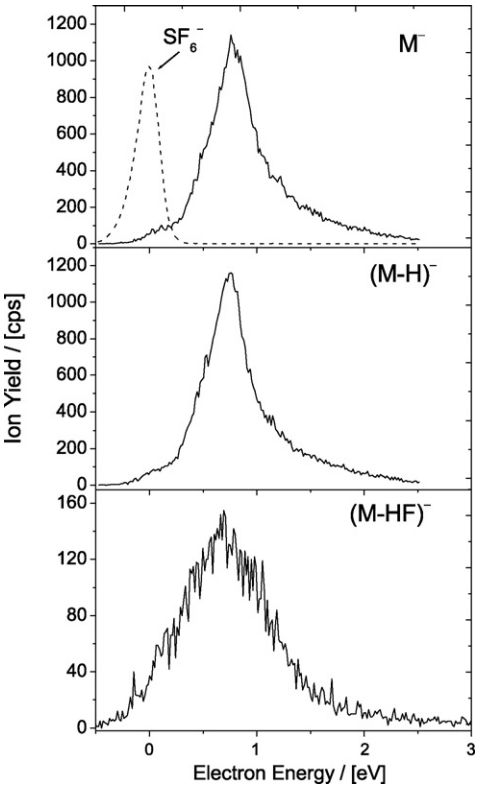

Fig. 3. Yield curves for the parent ion M^- ($CClF_2COOH^-$) and for the fragment ions $(M–H)^-$ and $(M–HF)^-$. $(M–H)^-$ and $(M–HF)^-$ are associated with the loss of the neutral hydrogen atom and neutral HF molecule, respectively. For comparison, the prototype system for associative attachment (SF_6) is also shown.

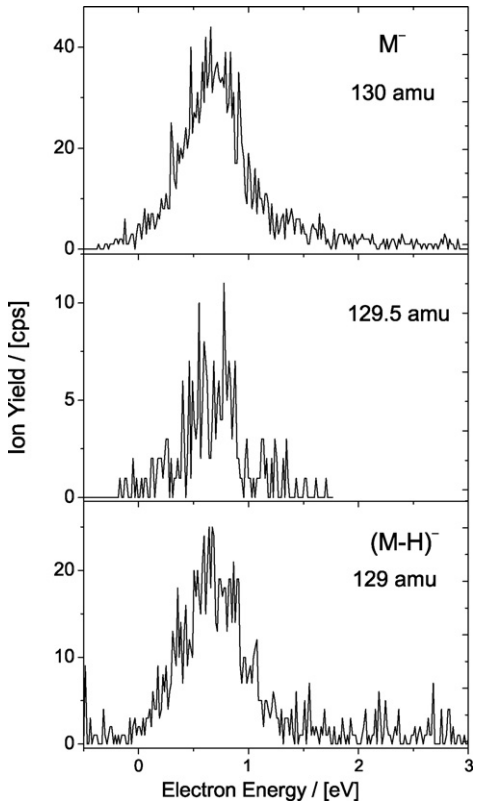

Fig. 4. Ion yields of M^- and $(M–H)^-$ and the signal between both mass units (129.5 amu) at improved mass resolution indicating that both ions can be separated and exhibit a very similar ion yield.

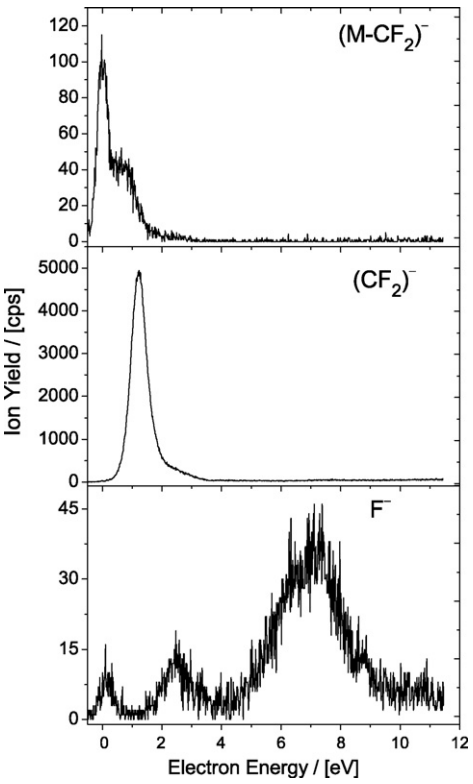

Fig. 5. Yields for the complementary ions $(M–CF_2)^-$ and CF_2^-, and for the atomic ion F^-.

Fig. 3 shows the non-decomposed metastable parent anion M^- on an expanded energy scale indicating its unusual behaviour as it is formed distinctly off 0 eV. At approximately the same energy the closed shell anion $(M–H)^-$ arising from the loss of a neutral hydrogen atom and also the ion due to the loss of neutral HF, $(M–HF)^-$, are generated. Fig. 4 demonstrates that the ions M^- and $(M–H)^-$ can in fact be separated and Fig. 5 finally presents three further fragments, the complementary pair $(M–CF_2)^-$ and CF_2^- and the atomic ion F^-, the latter indicating that the molecule also possesses resonances at higher energy. We observed further ions like OH^-, an ion due to the loss of CO_2, which is most likely the chlorofluromethane radical anion CHF_2Cl^-, an ion due to the loss of FCO_2 ($(CHFCl)^-$) and also the bihalide anion $FHCl^-$. The appearance of these fragmentation reactions will be included and discussed in a forthcoming treatment with the focus on electron-induced processes in condensed $CClF_2COOH$ [23].

3.2.1. Cleavage of the C–Cl bond

The two most intense ions arise from the cleavage of the C–Cl bond with the excess electron localised on either of the two fragments according to the DEA reactions:

$$e^- + CClF_2COOH \rightarrow CClF_2COOH^{-\#} \rightarrow CF_2COOH^- + Cl \quad (1a)$$

$$e^- + CClF_2COOH \rightarrow CClF_2COOH^{-\#} \rightarrow CF_2COOH + Cl^- \quad (1b)$$

with $CClF_2COOH^{-\#}$ the transient anion formed upon electron capture. Obviously, on going from CF_3COOH [12] to $CClF_2COOH$ the situation changes dramatically as the dominant loss of H (formation of CF_3COO^-) is now replaced by the cleavage of the C–Cl bond. Among the two complementary reactions (1a) and (1b) localisation of the excess charge on the larger polyatomic fragment (reaction (1a)) is by about one order of magnitude more favourable than formation of Cl^-. This observation may be rationalised by both energy and entropy (or phase space) arguments. From the energy point of view, the thermodynamic threshold for a single bond cleavage is given by the corresponding binding energy minus the electron affinity of the (neutral) fragment, on which the electron becomes localised. The fact that Cl^- is observed already close to 0 eV indicates that the C–Cl binding energy in the neutral parent molecule equals or is lower than the electron affinity of Cl (3.61 eV [24]). For the adiabatic electron affinity of the radical CHF_2COO we find the value 4.15 ± 0.16 eV [24] extracted from proton transfer equilibria [25] where the enthalpy of the dissociation process $CHF_2COOH \rightarrow CHF_2COO^- + H^+$ is determined. In the present DEA reaction (cleavage of the C–Cl bond) a closed shell compound with the structure $(CF_2COOH)^-$ is initially formed with the extra electron localised at the CF_2 site and we have no information on its energy with respect to the constitutional isomer $(CHF_2COO)^-$. It is also possible, that in a slow DEA process rearrangement in the transitory precursor anion finally generates CHF_2COO^-, should this be the more stable isomer. At least in the range of 0.75 eV DEA obviously competes with formation of the metastable parent anion (Figs. 2–5). Apart from energy arguments it is obvious that the probability for electron localisation on the compound CF_2COOH consisting of seven atoms is higher than on the single Cl atom which explains that (1a) is more intense than (1b).

3.2.2. Formation of the metastable parent anion and loss of neutral H and neutral HF

A very interesting point concerns the peculiarities in the formation of the non-decomposed parent anion in the way that (i) it is formed within a resonant feature distinctly off 0 eV (0.75 eV) and (ii) the fact that the target molecule is of only low symmetry and exhibits DEA features at even lower energies. The common picture to rationalise the formation of metastable parent anions by capture of free electrons under collision free conditions is based on the idea that the electronic energy of the electron attaching system (comprised of the energy of the incoming electron and the electron affinity of the molecule) is effectively dispersed over the vibrational degrees of freedom in the parent anion, thereby delaying autodetachment [26]. A prototype system of resonant associative attachment is SF_6, which possesses one of the highest electron attachment cross-sections associated with a very narrow resonance near 0 eV [22,27]. In SF_6, all DEA channels are endothermic and hence not accessible at 0 eV (provided that the temperature of the target molecule is low), i.e., DEA does not compete with autodetachment. There are many further examples of metastable parent anion formation like in perfluorobenzene [28] and other aromatic compounds [29] including the explosives trinitrotoluene (TNT) [30] or dinitrobenzene (DNB) [31]. In all cases formation of M^- is restricted to a comparably narrow energy range close to zero. In the explosives, DEA competes with metastable anion formation. There are only a few exceptions of parent anion formation beyond 0 eV, namely the anion of p-benzoquinone at 1.4 eV [32,33,34], azobenzene at 0.9 and 1.2 eV [35] and pyromellitic acide amide at 1.65 eV [36]. Electron attachment to C_{60} is a particular case generating C_{60}^- over a wide and structured feature extending from threshold (0 eV) to about 12 eV [37,38,39]. C_{60} is a highly symmetric compound with equal binding energies for each C atom thereby providing ideal conditions for a delayed autodetachment resulting in a situation that C_{60}^- can be observed on the mass spectrometric time scale at attachment energies up to 12 eV.

In contrast, the present system behaves completely different as here the dominant DEA reactions take place close to 0 eV while formation of the parent anion occurs within a resonant feature peaking at 0.75 eV. At that energy, some of the fragment ions arising from DEA have also a peak like $(M–H)^-$ and $(M–HF)^-$ (Fig. 3) or $(M–CF_2)^-$ (Fig. 5).

One may qualitatively interpret such behaviour by invoking two different electronic states, one located near 0 eV and the second near 0.75 eV. While the low energy shape resonance possesses dis-

tinct σ^*(C–Cl) character thereby leading to prompt dissociation, the resonance at 0.75 eV is characterised by an MO which is more extended over the molecule, most likely having some π^*(COOH) character. In this case, strong coupling of electronic with vibrational energy delays autodetachment into the μs time domain which is the observation window in the present experiment. Formation of the non-decomposed anion obviously competes with various DEA channels as seen on the shoulder on the complementary ions $(M–Cl)^-$ and Cl^- near 0.7 eV (Fig. 2) or the ions in Figs. 3 and 5. While in Fig. 3 the $(M–H)^-$ signal carries some intensity from the adjacent ion M^-, both ions can be separated by operating the quadrupole at higher mass resolution with the disadvantage of lower intensity. This is shown in Fig. 4 where the signal intensity between the masses of M^- and $(M–H)^-$ (129.5 amu) is much lower indicating a nearly complete separation. It should be noted that abstraction of HF is a quite complex process associated with the cleavage of two bonds, hydrogen transfer, and formation of the HF molecule. Apart from the detailed energetic situation (which is not completely available from established thermodynamic data) it is obvious that the neutral counterpart of the ion $CClFCOO^-$ ($(M–HF)^-$) must in fact be HF (and not H + F) since the ion is already observed below 1 eV.

It should finally be mentioned that the parent anion M^- could principally also be the result of initial electron attachment to a dimer. As mentioned above, the presence of a small amount of dimers cannot completely be ruled out. If dimers or larger homologues would be present, one would expect the presence of solvated fragment ions of the form $M{\cdot}Cl^-$ with a signal intensity much stronger than that of M^- [40].

3.2.3. The complementary ions CF_2^- and $(M–CF_2)^-$ and formation of F^-

The complementary ion pair can be considered to formally arise from the DEA reactions:

$$e^- + CClF_2COOH \rightarrow CClF_2COOH^{-\#} \rightarrow CF_2^- + ClCOOH \quad (2a)$$

$$e^- + CClF_2COOH \rightarrow CClF_2COOH^{-\#} \rightarrow CF_2 + ClCOOH^- \quad (2b)$$

which would require excision of the CF_2 unit from the TNI and transfer of the Cl atom to the COOH unit to form chloroformic acid. Interestingly, reaction (2a) is by more than one order of magnitude more intense than (2b) the former having a resonance peak at 1.2 eV. While CF_2 and its anion are well known as thermodynamically stable compounds, chloroformic acid is an unstable species [41,42]. It can be produced by flash photolysis in a mixture of Cl_2 and HCOOH and from rapid-scan infrared spectroscopy its lifetime was estimated to be 50–70 μs under the conditions of the corresponding experiment [43]. In light of that one can expect that the neutral component in reaction (2a) will lead to the stable compounds HCl + CO_2. *Ab initio* calculations [42] in fact predict the decomposition of chloroformic acid into HCl + CO_2 to be exothermic by about −1.0 eV.

On the other hand in reaction (2b) the mass spectrometer is set to detect an anion of the stoichiometric composition $(HClCO_2)^-$ which could be the anion of chloroformic acid. Formic acid itself does not possess a positive adiabatic electron affinity [1] and the low intensity of $ClCOOH^-$ suggests, that this compound is also unstable, and most likely with respect to both, electron loss and dissociation. In the case that the excess electron in $(HClCO_2)^-$ would exist in a bounds state, the anionic system would detach the extra electron in the course of dissociation since neither HCl nor CO_2 can bind an extra electron in a thermodynamically stable state.

The yield of F^- finally shows that the molecule possesses a broad resonance feature in the range between about 5–9 eV. This feature may be composed of different and energetically overlapping resonances. It is likely that these features represent core excited resonances, i.e., electronically excited anions with two electrons in normally unoccupied MOs. It will be shown in a forthcoming manuscript, that this high-energy feature is relevant in the electron-induced desorption (ESD) of anions from nanofilms and also the electron stimulated production of CO_2 in nanofilms [23].

The F^- ion yield shows also a signal right at the threshold (near 0 eV). Since the C–F bond energy is larger than the electron affinity of the F atom [24], it cannot be the result of DEA to ground sate $CClF_2COOH$. On the other hand, such threshold F^- signals are sometimes observed in DEA [17] and can be due to transitions from vibrationally excited molecules (hot bands) [44]. They can also be due to artifacts like (dissociative) electron attachment to fragments produced by thermal decomposition at the hot filament or simply very small impurities. Due to the reciprocal energy dependence of the cross-section for electron attachment such effects can cause measurable signals at zero energy even when the concentration of the corresponding precursor molecule is negligibly small (i.e., negligibly small impurity or negligibly small population of vibrationally excited states).

3.3. Attachment rate constant and attachment cross-section

The attachment rate constant (k) obtained in the swarm experiment is connected to the attachment cross-section (σ) by

$$k = \int_0^\infty f(\upsilon)\upsilon\sigma(\upsilon)\, d\upsilon \quad (3)$$

with $f(\upsilon)$ the normalised velocity distribution of the electrons at the respective temperature. By using the averaged quantities:

$$k = \langle\sigma\rangle\,\langle\upsilon\rangle \quad (3a)$$

and taking $\langle\upsilon\rangle$ from a standard Maxwell–Boltzmann distribution ($\langle\upsilon\rangle \approx 10^7\,cm\,s^{-1}$ at 300 K) and k from above we obtain $\langle\sigma\rangle \approx 1.5 \times 10^{-17}\,cm^2$ for the attachment of *thermal* electrons to $CClF_2COOH$.

One has to be careful, however, when directly transferring the rate constant from the swarm experiment into a cross-section in the beam experiment due to the inherently different conditions. While the beam experiment operates under single collision conditions, in the swarm experiment the intermolecular collision frequencies are in the range between about 4×10^9 to $1.5 \times 10^9\,s^{-1}$ corresponding to an average time between two collisions between 250 ps down to nearly 1 ns. This is a time scale much shorter than the observation window for the metastable parent anion in the beam experiment. Generally, intermolecular collisions can remove electronic and vibrational energy thereby suppressing autodetachment *and* dissociation. Since the swarm experiments measure the *disappearance* of free electrons and since the rate constant is independent of the pressure one can conclude that autodetachment does not change in the pressure range covered. On the other hand, since the time between collisions is small compared to the lifetime of the TNI (*vide supra*) it is likely that in the swarm experiment the intensity of the DEA channels is suppressed in favour of the formation of non-decomposed anions.

4. Conclusion

Chlorodifluoroacetic acid ($CClF_2COOH$) possesses a strong resonance feature close to 0 eV which primarily decomposes by the cleavage of the C–Cl bond with the excess charge localised on either of the fragments CF_2COOH^- ($(M–Cl)^-$) or Cl^-. This behaviour differs substantially from the analogues trifluoroacetic acid (CF_3COOH) [12] or acetic acid (CH_3COOH) [2] which both decompose primarily via the loss of a neutral hydrogen atom via a low energy resonance located at 0.5 eV (CF_3COOH) and 1.5 eV (CH_3COOH) thereby generating the closed shell anion $(M–H)^-$. The most unexpected

and striking feature is the observation of the non-decomposed parent anion M^- which is generated within a resonant feature located at 0.75 eV. Under collision free conditions, parent negative ions formed by attachment of free electrons are in principle unstable towards autodetachment and hence such metastable transients are usually observed only at electron energies close to 0 eV. From electron swarm measurements the rate constant for the attachment of thermal electrons to ($CClF_2COOH$) is determined as $k = 1.5 \times 10^{-10}$ cm^3 molec.$^{-1}$ s^{-1}.

Acknowledgments

This work has been supported by the Polish Ministry of Science and Higher Education, the Deutsche Forschungsgemeinschaft (DFG), the Fonds der Chemischen Industrie and the Freie Universität Berlin. JK acknowledges support for a visit to Berlin from the European Union via the COST action CM0601 (Electron Controlled Chemical Lithography, ECCL) and CKL acknowledges support from DFG for a visit to Siedlce.

References

[1] A. Pelc, W. Sailer, P. Scheier, M. Probst, N.J. Mason, E. Illenberger, T.D. Märk, Chem. Phys. Lett. 361 (2002) 277.
[2] W. Sailer, A. Pelc, M. Probst, J. Limtrakul, P. Scheier, E. Illenberger, T.D. Märk, Chem. Phys. Lett. 378 (2003) 250.
[3] S. Gohlke, A. Rosa, F. Brüming, M.A. Huels, E. Illenbereger, J. Chem. Phys. 116 (2002) 10164.
[4] I. Martin, T. Skalicky, J. Langer, H. Abdoul-Carime, G. Karwasz, E. Illenberger, M. Stano, S. Matejcik, Phys. Chem. Chem. Phys. 7 (2005) 2212.
[5] D.F. McMillen, D.M. Golden, Ann. Rev. Phys. Chem. 33 (1982) 493.
[6] T.G. Clements, R.G. Continetti, J. Chem. Phys. 115 (2001) 5345.
[7] T.G. Clements, R.G. Continetti, J.S. Francisco, J. Chem. Phys. 117 (2002) 6478.
[8] K. Aflatooni, B. Hitt, G.A. Gallup, P.D. Burrow, J. Chem. Phys. 115 (2001) 6489.
[9] T. Rescigno, C.S. Trevisan, A.E. Orel, Phys. Rev. Lett. 96 (2006) 213201.
[10] M. Allan, J. Phys. B 39 (2006) 2939.
[11] G.A. Gallup, P.D. Burrow, I.I. Fabrikant, Phys. Rev. A 79 (2009) 042701.
[12] J. Langer, M. Stano, S. Gohlke, V. Foltin, S. Matejcik, E. Illenberger, Chem. Phys. Lett. 419 (2006) 228.
[13] F.A. Gianturco, R.R. Lucchese, J. Langer, I. Martin, M. Stano, G. Karwasz, E. Illenberger, Eur. Phys. J. D 35 (2005) 417.
[14] J. Langer, I. Martin, G. Karwasz, E. Illenberger, Int. J. Mass Spectrom. 249–250 (2006) 477.
[15] M. Allan, Phys. Rev. Lett. 98 (2007) 123201.
[16] J. Kopyra, J. Wnorowska, M. Foryś, I. Szamrej, Int. J. Mass Spectrom. 268 (2007) 60.
[17] R. Balog, J. Langer, S. Gohlke, M. Stano, H. Abdoul-Carime, E. Illenberger, Int. J. Mass Spectrom. 233 (2004) 267 (Review Article).
[18] A. Stamatovic, G.J. Schulz, Rev. Sci. Instrum. 41 (1970) 423.
[19] A.S. Coolidge, J. Am. Chem. Soc. 52 (1930) 1874.
[20] W. Barszczewska, J. Kopyra, J. Wnorowska, I. Szamrej, J. Phys. Chem. 107 (2003) 11427.
[21] L.G. Christophorou, Z. Phys. Chem. 195 (1996) 195.
[22] L.G. Christophorou, J.K. Olthoff, Fundamental Electron Interactions with Plasma Processing Gases, Kluwer Academic, New York, 2004.
[23] M. Orzol, J. Kopyra, C. König-Lehmann, E. Illenberger, in preparation.
[24] The NIST chemistry webbook: http://webbook.nist.gov/chemistry.
[25] G. Caldwell, R. Renneboog, P. Kebarle, Can. J. Chem. 67 (1989) 661.
[26] E. Illenberger, Electron attachment processes in free and bound molecules, in: C.-Y. Ng (Ed.), Photoionization. Part II. Advanced Series in Physical Chemistry, vol. 10B, World Scientific, Singapore, 2000, pp. 1063–1160.
[27] D. Klar, M.-W. Ruf, H. Hotop, Int. J. Mass Spectrom. 205 (2001) 93.
[28] M. Fenzlaff, E. Illenberger, Chem. Phys. 136 (1989) 443.
[29] L.G. Christophorou, D.L. McCorkle, A.A. Christodoulides, Electron attachment processes, in: L.G. Christophorou (Ed.), Electron–Molecule Interactions and their Applications, Academic Press, Orlando, 1984.
[30] P. Sulzer, F. Rondino, S. Ptasinska, E. Illenberger, T.D. Märk, Paul Scheier, Int. J. Mass Spectrom. 271 (2008) 149–153.
[31] P. Sulzer, A. Mauracher, S. Denifl, M. Probst, T.D. Märk, P. Scheier, E. Illenberger, Int. J. Mass Spectrom. 266 (2007) 138.
[32] L.G. Christophorou, J.G. Carter, A.A. Christodoulides, Chem. Phys. Lett. 3 (1969) 237.
[33] C.D. Cooper, W.T. Naff, R.N. Compton, J. Chem. Phys. 63 (1975) 2752.
[34] J. Allan, Chem. Phys. 81 (1983) 3235.
[35] Y.V. Vasilïev, V.A. Mazunov, E.R. Nazirov, Org. Mass Spectrom. 26 (1991) 739.
[36] O.G. Khvostenko, G.M. Tuimedov, Rapid Commun. Mass Spectrom. 20 (2006) 3699.
[37] Th. Jaffke, E. Illenberger, M. Lezius, St. Matejcik, D. Smith, T.D. Märk, Chem. Phys. Lett. 226 (1994) 213–218.
[38] S. Matejcik, T.D. Märk, P. Spanel, D. Smith, Th. Jaffke, E. Illenberger, J. Chem. Phys. 102 (1995) 2516–2521.
[39] O. Elhamidi, J. Pommier, R. Abouaf, J. Phys. B Atom. Mol. Opt. Phys. 30 (1997) 4633.
[40] E. Illenberger, Chem. Rev. 92 (1992) 1589.
[41] R.J. Jensen, G.C. Pimentel, J. Phys. Chem. 71 (1967) 1803.
[42] J.S. Francisco, W.A. Ghoul, Chem. Phys. 157 (1991) 89.
[43] K.C. Herr, G.C. Pimentel, Appl. Opt. 4 (1965) 25.
[44] I. Hahndorf, E. Illenberger, Int. J. Mass Spectrom. Ion Proc. 167/168 (1997) 87.